Engineerable compression of ultrashort pulses by use of second-harmonic generation in chirped-period-poled lithium niobate

M. A. Arbore

E. L. Ginzton Laboratory, Stanford University, Stanford, California 94305

A. Galvanauskas and D. Harter

IMRA America, 1044 Woodridge Avenue, Ann Arbor, Michigan 48105

M. H. Chou and M. M. Fejer

E. L. Ginzton Laboratory, Stanford University, Stanford, California 94305

Received May 7, 1997

We demonstrate the use of an aperiodic quasi-phase-matching (QPM) grating to generate second-harmonic pulses that are stretched or compressed relative to input pulses at the fundamental frequency. We frequency doubled an externally chirped erbium-doped fiber laser generating 17-ps (FWHM) pulses at 1560 nm to produce near-transform-limited 110-fs (FWHM) pulses at 780 nm by use of a 5-cm-long lithium niobate crystal poled with a QPM grating chirped from an 18.2- to a 19.8-μm period. © 1997 Optical Society of America

Ultrafast laser systems require control of dispersion for delivery of chirp-free ultrashort pulses; several methods for stretching and compressing optical pulses by use of dispersive linear systems[1,2] are in common use. Nonlinear-optical frequency conversion, especially second-harmonic generation[3] (SHG), is also widely used, extending the wavelength range that is accessible to ultrafast laser systems. Recently it was shown theoretically[4] that a chirped-grating quasi-phase-matched QPM second-harmonic (SH) generator can provide significant effective dispersion at the SH wavelength relative to the fundamental wavelength, eliminating the need for dispersive delay lines in some ultrafast laser systems. These monolithic devices are far more compact than diffraction-grating-based or prism-based dispersive delay lines and offer high power-handling capability.

In this Letter we demonstrate simultaneous 150-fold pulse compression and SHG, using an externally chirped erbium-doped fiber laser and chirped-period-poled lithium niobate (CPPLN) for quasi-phase-matched SHG; 110-fs (FWHM) near-transform-limited pulses at the SH frequency are generated from 17-ps pulses at the fundamental frequency. Results are in good agreement with numerical predictions based on square spectra and show clear qualitative agreement with a previously published analytical model[4] based on Gaussian spectra.

Quasi-phase matching[5] (QPM) brings broad engineerability to the phase-matching properties of frequency-conversion devices but has, to date, been applied almost exclusively with periodic gratings. Such use of QPM[6,7] has permitted interactions with combinations of noncritical phase matching, large nonlinear coefficients, and spectral coverage that are not available with birefringent phase matching. The use of aperiodic QPM gratings for increasing the wavelength acceptance bandwidth[8–10] in cw SHG has been studied, but the implications of the phase response of chirped QPM structures to the field of ultrashort-pulse frequency conversion have not yet been investigated experimentally.

The theory of pulse compression during SHG in chirped QPM gratings is described in detail in Ref. 4; here we summarize the principal concepts and terminology. The chirp in the QPM grating causes an effect analogous to group-velocity dispersion (GVD). This effect does not disperse the input fundamental pulse but directly generates a SH pulse that is stretched or compressed. This effective GVD is a result of the interplay of two phenomena: group-velocity mismatch between the fundamental and the SH pulses, which is intrinsic to the nonlinear material, and spatial localization of SHG of particular frequency components, which is a property of chirped QPM gratings. Different spectral components of the fundamental pulse are frequency doubled at different locations in the chirped QPM grating, and therefore the SH's of these different spectral components experience a different time delay relative to the fundamental pulse. The GVM parameter is $\delta \equiv ({\nu_{g_1}}^{-1} - {\nu_{g_2}}^{-1})$, where ν_{g_1} and ν_{g_2} are the group velocities of the fundamental and the SH pulses, respectively. In lithium niobate, $\delta = 0.30$ ps/mm for SHG of a 1560-nm fundamental.

In the frequency domain, undepleted-pump plane-wave QPM SHG of ultrashort pulses under conditions in which intrapulse GVD can be neglected can be described by the simple transfer-function relation

$$\hat{A}_2(\Omega) = \hat{D}(\Omega)\widehat{A_1^2}(\Omega). \qquad (1)$$

In Eq. (1), $\Omega = \omega - \omega_m$ is the detuning of the angular frequency from the spectral center of the pulse, where

0146-9592/97/171341-03$10.00/0

$\omega_m = \omega_1$ or $\omega_m = \omega_2 = 2\omega_1$ for the fundamental or the SH pulse, respectively. $\hat{A}_2(\Omega)$ is the Fourier transform of the SH pulse, $A_1^2(\Omega)$ is the Fourier transform of the square of the fundamental pulse, and $\hat{D}(\Omega)$ is a QPM transfer function related to the cw SHG tuning curve.

For QPM SHG, the **k** vector of the QPM grating must satisfy $k_{\text{grating}} = 4\pi(n_2 - n_1)/\lambda_1$, where λ_1 is the fundamental wavelength and the refractive indices n_1 and n_2 are evaluated at the fundamental and the SH frequencies, respectively. The period of the QPM grating is given by $\Lambda_{\text{grating}} = 2\pi/k_{\text{grating}}$. The effective linear GVD of a chirped QPM grating can be described by the parameter D_{g_2}, where

$$D_{g_2} = \frac{1}{2}\frac{\mathrm{d}}{\mathrm{d}z}k_{\text{local}}(z), \tag{2}$$

where $k_{\text{local}}(z)$ is the local grating **k** vector. In Ref. 4 it is shown that for sufficiently long crystals $\hat{D}(\Omega) \propto \exp(i\Omega^2\delta^2/4D_{g_2})$, indicating that the SH experiences an effective GVD of $\delta^2/2D_{g_2}$ (and can be compressed) relative to the fundamental pulse. Describing the input pulse by its chirp rate $1/D_p$, we note that there is an optimum pulse for maximum compression:

$$D_p = -\delta^2/D_{g_2} \equiv D_{p,\text{opt}}. \tag{3}$$

The maximum duration of input pulses that can be entirely compensated is limited by the length of the nonlinear material and its group-velocity-mismatch parameter, whereas the minimum duration of output pulses that can be generated is limited by the input-pulse bandwidth and by uncompensated high-order dispersion (although the latter can be corrected with more-complicated aperiodic QPM gratings).

The 5-cm-long sample of CPPLN used in this experiment was fabricated by full-wafer electric-field poling[11] and had local QPM periods that varied linearly from 18.2 to 19.8 μm ($D_{g_2} \cong 0.28\ \text{mm}^{-2}$). The SHG acceptance bandwidth was measured with a tunable cw source to be ~50 nm; thus the sample is capable of generating SH pulses with up to a 25-nm bandwidth.

We self-phase modulated the output from an amplified erbium-doped fiber laser to produce pulses at a 20-MHz repetition rate and with 75-nm-wide, approximately square spectra with a center wavelength of 1560 nm. We stretched these pulses with a diffraction-grating delay line containing a telescope in the Martinez configuration[2] to provide continuously variable dispersion. The diffraction grating had 830 lines/mm and was oriented at 32° to the incident beam. The delay line had negligible high-order dispersion. The fundamental beam was loosely focused through the sample to a spot with $1/e$ electric-field radius of 100 μm. The autocorrelations and the spectra of the fundamental and the SH pulses were measured before and after the CPPLN crystal, respectively. The SH spectra typically had a 16-nm-wide squarelike shape for various pulse lengths, consistent with the observed triangular autocorrelations for the stretched SH pulses.

Figure 1 shows an autocorrelation trace of the SH pulses for $D_p = 0.29\ \text{ps}^2$, giving an autocorrelation width of 150 fs. The square-shaped SH spectrum has a deconvolution factor of 0.75, implying pulse durations of 110 fs (FWHM). The theoretical FWHM pulse duration for transform-limited, 16-nm-wide (at 780 nm) spectra is 105 fs, indicating that, at least in the low conversion-efficiency limit, negligible undesired high-order chirp is introduced by the nonlinear interaction. The input of the fundamental pulses to the CPPLN sample under these conditions had durations (and autocorrelations widths) of 17 ps (FWHM).

To demonstrate more clearly the effective GVD properties of chirped QPM gratings, we measured autocorrelation widths for the input fundamental pulses and the output SH pulses for various delay line positions; the results are shown in Fig. 2. The fundamental pulse FWHM duration was varied from 1 ps (with net negative dispersion) to 95 fs at zero dispersion to 19 ps (with net positive dispersion). The solid curves matching the autocorrelation data are the numerically evaluated autocorrelation widths for square (75 nm wide at 1560 nm or 16 nm wide at 780 nm)

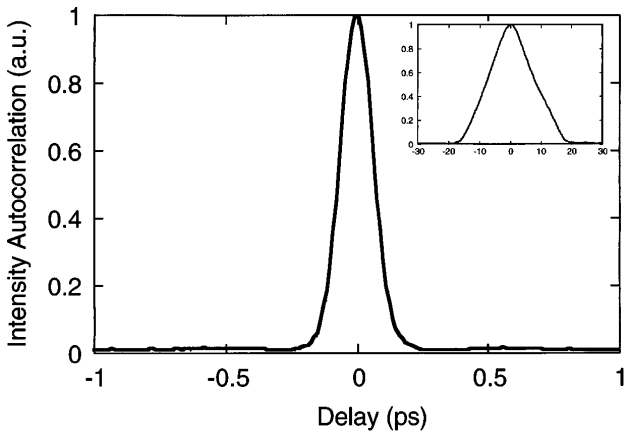

Fig. 1. SH autocorrelation trace at maximum compression, indicating 110-fs (FWHM) duration. The input fundamental pulses (inset autocorrelation) that gave rise to this SH output had durations of 17 ps (FWHM).

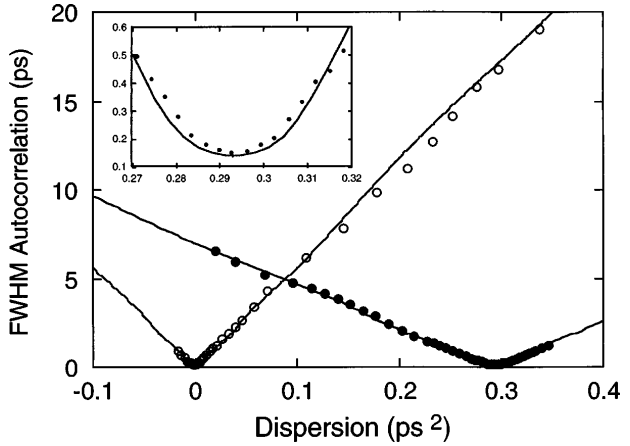

Fig. 2. Input (open circles) and output (filled circles) autocorrelation widths plotted against the chirp of the input pulse (expressed in terms of delay line GVD) for SHG in a chirped QPM grating with $D_{g_2} \cong 0.28\ \text{mm}^{-2}$. The curves are theoretical predictions based on square spectra with 75-nm width at 1560 nm (near open circles) and 16-nm width at 780 nm (near closed circles). The inset shows the output-pulse autocorrelations near maximum compression.

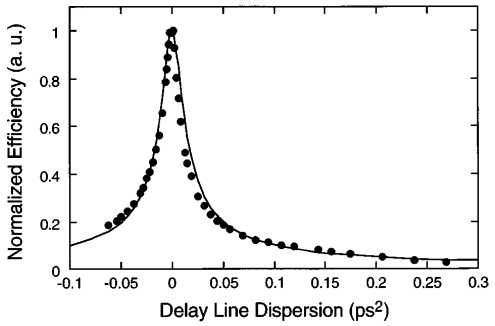

Fig. 3. Efficiency plotted against delay line dispersion. The curve is a plot of theoretical efficiency approximated by that for pulses with a 25-nm (FWHM) Gaussian fundamental spectrum (18-nm SH spectrum), normalized to the peak experimental value.

spectra. The inset in Fig. 2 shows the SH autocorrelation widths near the maximum compression point. The width of the SH spectrum is approximately 65% of that permitted by the phase-matching bandwidth of the CPPLN sample. We attribute this spectral narrowing to the nonideal chirp in the wings of the fundamental pulse spectra (resulting from the use of self-phase modulation to increase the pulse bandwidth) and to the spatial chirp in one transverse dimension of the fundamental beam (resulting from the simple single-grating design of the Martinez pulse compressor). The use of cleaner input fundamental pulses stretched in optical fiber would alleviate both experimental limitations. The difference in the slope of the SH autocorrelation curve relative to the slope of the fundamental autocorrelation curve reflects the fact that the SH spectrum did not possess precisely twice (half) the frequency (wavelength) bandwidth of the fundamental pulse.

The SH pulses had a minimum duration when $D_p = 0.29\ \mathrm{ps}^2$ (experimental uncertainty of $\sim 5\%$), which is in reasonable agreement with $D_{p,\mathrm{opt}} = 0.33\ \mathrm{ps}^2$ as predicted by Eq. (3) neglecting GVD. The sign of $D_{p,\mathrm{opt}}$ depended, as expected, on the sample orientation, and the magnitude of $D_{p,\mathrm{opt}}$ scaled approximately with D_{g_2} when other CPPLN crystals were substituted.

Figure 3 shows the normalized average-power conversion efficiency measured at low absolute efficiencies (i.e., low-energy pump) and plotted against the chirp of the input pulses. The solid curve in Fig. 3 is a fit to Eq. (13) of Ref. 4, which gives the theoretical efficiency for a dispersed Gaussian pulse; this simple analytical form was used because the experimental conditions described above precluded more-detailed calculation of the efficiency. The highest conversion efficiency observed was 110%/nJ, comparable with that which can be obtained with unchirped periodically poled lithium niobate and roughly half that expected for optimal experimental conditions. Although the normalized conversion efficiency decreases inversely with the stretching ratio, this decrease is typically offset by pulse energies that increase with the stretching ratio. Preliminary experiments indicate that as high as 40% absolute efficiencies can be observed for stretched fundamental pulse energies in the nanojoule range.

Chirped QPM gratings provide degrees of freedom that are not found with other pulse-compression devices. The gratings are monolithic, alignment is simple, and significant effective GVD's can be implemented in minimal volume. Because of the lithographically defined nature of the grating structure, arbitrary high-order GVD compensation is also simple to implement through the design of the lithography mask. Unlike in most frequency-conversion schemes, for sufficiently long devices the chirped QPM grating is inherently tunable without adjustment of temperature or alignment.

In summary, we have shown that chirped quasi-phase-matching gratings can be used for simultaneous second-harmonic generation and ultrashort pulse compression. We have generated 110-fs (FWHM) near-transform-limited pulses with 150-fold compression relative to the input pulses; output-pulse duration and efficiency results are in good agreement with expectations. In future theoretical and experimental research we plan to address effects arising from pump depletion and intrapulse GVD as well as the application of chirped QPM gratings to other frequency-conversion interactions, such as parametric amplification and oscillation. Current results show that a compact, monolithic, and efficient pulse compressor exhibiting arbitrary phase correction can be implemented in a simple device.

This research was supported by the Advanced Research Projects Agency through the Center for Nonlinear Optical Materials and by the Joint Services Electronics Program. The authors thank Crystal Technology for its generous donation of $LiNbO_3$ substrates and M. E. Fermann for assistance with early stages of the experiment.

References

1. G. C. Dieles and W. Rudolph, *Ultrashort Laser Pulse Phenomena* (Academic, New York, 1996).
2. O. E. Martinez, IEEE J. Quantum Electron. **QE-23,** 59 (1987).
3. S. A. Akhamanov, in *Quantum Electronics: A Treatise*, H. Rabin and C. L. Tang, eds. (Academic, New York, 1975), Vol. 1, part B, pp. 476–586.
4. M. A. Arbore, O. Marco, and M. M. Fejer, Opt. Lett. **22,** 865 (1997).
5. M. M. Fejer, G. A. Magel, D. H. Jundt, and R. L. Byer, IEEE J. Quantum Electron. **28,** 2631 (1992).
6. V. Pruneri, S. D. Butterworth, and D. C. Hanna, Opt. Lett. **21,** 390 (1996).
7. M. A. Arbore, M. M. Fejer, M. E. Fermann, A. Hariharan, A. Galvanauskas, and D. Harter, Opt. Lett. **22,** 13 (1997).
8. T. Suhara and H. Nishihara, IEEE J. Quantum. Electron. **26,** 1265 (1990).
9. M. L. Bortz, M. Fujimura, and M. M. Fejer, Electron. Lett. **30,** 34 (1994).
10. K. Mizuuchi, K. Yamamoto, M. Kato, and H. Sato, IEEE J. Quantum Electron. **30,** 1596 (1994).
11. L. E. Myers, R. C. Eckardt, M. M. Fejer, R. L. Byer, W. R. Bosenberg, and J. W. Pierce, J. Opt. Soc. Am. B **12,** 2102 (1995).